University of Tehran Press

DESERT

Online Issn: 475-2345X

Home page: https://jdesert.ut.ac.ir/

Evaluation of the classification accuracy of NDVI index in the preparation of land cover map

Mohammad Mansourmoghaddam[1], Iman Rousta[2], Hamid Reza Ghafarian[2]✉

1- Center for Remote Sensing and GIS studies, Shahid Beheshti University, Tehran, Iran
2- Department of Geography, Yazd University, Yazd, Iran. Email: hrghafarian@yazd.ac.ir

Article Info

Article type:
Research Article

Article history:

Received 18 February 2022

Received in revised form 24 March 2022

Accepted 2 August 2022

Published online 25 September 2022

Keywords:
Landsat 8,
Threshold,
Normalized Difference Vegetation Index,
Satellite Image Classification

ABSTRACT

The preparation of land cover maps provides the possibility of studying the impact of land surface changes on sustainable development and is significant for a wide range of important issues at the global level. The current research aims to facilitate the preparation of land cover maps using the classification of Normalized Difference Vegetation Index (NDVI) values and prepare land cover maps from it. For this purpose, first, two complete consecutive Landsat-8 scenes of parts of Iran and Turkmenistan were selected for August 30, 2021. Then the images were classified using supervised classification algorithms including Neural Network Classification (NNC), maximum Likelihood Classification (MLC), Support Vector Machine (SVM), Minimum Distance (MinD) and Mahalanobis Distance (MahD). In the next step, to perform an evaluation, by using a thousand ROI for a test, the overall accuracy, kappa coefficient, user accuracy and producer accuracy of the map produced by each of the algorithms were calculated. Then, using the most optimal algorithm, the threshold of NDVI image values was extracted in order to classify it and the obtained map was re-evaluated for accuracy. Among the evaluated algorithms, the MLC algorithm had the most optimal performance with a kappa coefficient of 0.75 and overall accuracy of 80.86%. The results of evaluating the accuracy of the NDVI Based land cover Classification (NBC) index also indicated that this map has extracted the land cover map with an overall accuracy of 83% and a Kappa coefficient of 0.77. This index showed good performance in the classification of Bare Land Class (BLC), Water Area Class (WAC) and Salt Marsh Class (SMC) with user accuracy and producer accuracy above 94%. This is while the Agricultural Land Class (ALC) and Vegetation Class (VC) were classified by this index with producer accuracy of above 73% and user accuracy of 69% and 97%, respectively. The results of this research indicate the acceptable accuracy of NDVI index values for the production of natural land cover maps and can be used in order to prepare these maps for geographic monitoring and achieving sustainable environmental development.

Cite this article: M. Mansourmoghaddam, I. Rousta &Ghafarian H. (2022). Evaluation of the classification accuracy of NDVI index in the preparation of land cover map. DESERT, 27 (2), DOI: 10.22059/jdesert.2022.90834

 DOI: 10.22059/jdesert.2022.90834

Introduction

Remote sensing techniques and multi-spectral satellite images are very efficient to obtain a better understanding of the Earth's environment (Alavipanah *et al*., 2022). Remote sensing is the science and art of obtaining information and extracting spectral, spatial and temporal characteristics of objects, regions, or terrestrial phenomena such as vegetation, urban areas, agricultural lands and water resources without physical contact with them (Hacihaliloglu & Karta, 2004). Remote sensing data has many applications including land cover classification, soil moisture measurement, forest type classification, vegetation water content measurement, snow mapping, ice type classification and oceanography, etc. (Hacihaliloglu & Karta, 2004).

Preparing maps and studying land cover and preparing maps change is significant for a wide range of globally important issues, such as finding changes in different periods, obtaining quantitative data about land uses, etc. Because land cover changes affect the earth's surface and have leading consequences for sustainable development and livelihood systems (Turner *et al*., 1995). Image classification is one of the methods of detecting phenomena on images, based on statistical methods, reflective characteristics of phenomena. One of the classification methods is its supervised type, and it is a process in which the user selects some samples for each land cover class on the image, which are called training samples. This type of land cover classification is based on the spectral signature specified in the algorithm training. Image classification algorithms determine each class as similar to the one in the training set. In supervised classification, the NDVI image is classified into certain classes according to its value (Taufik *et al.*, 2016).

Many algorithms have been developed to remotely estimate the biophysical properties of vegetation, in terms of spectral band composition, spectral reflectance derivatives, neural networks, inverse radiation transfer models, and several unique multispectral statistical methods. However, the most widely used type of algorithm is the mathematical combination of visible and near-infrared reflectance bands, in the form of spectral vegetation indices (Taufik *et al*., 2016). The vegetation index, as one of the outputs of multi-spectral remote sensing images, can be used as an index to quantify the greenness of plants by satellite data. Among the many vegetation indices, the Normalized Difference Vegetation Index (NDVI) has been used more (Rouse Jr *et al*., 1973). By analyzing images at near-infrared and red wavelengths, researchers can determine vegetation cover on Earth's surface (Taufik *et al*., 2016).

Several studies have used the NDVI index to classify and distinguish different types of land covers and facies. Among them, the research of Silakhori and Ownegh (Silakhori & Ownegh, 2018) who used the NDVI index in highlighting, identifying, and distinguishing the geomorphological facies of Sabzevar in Iran can be mentioned. In another study, Mohammadnazhad *et al*. (Mohammadnazhad *et al*., 2022) used the NDVI index as the most appropriate index for modeling vegetation forms in order to model the primary production of the land surface and the vegetation forms of the Siah Posh and Ganjgah pastures of Ardabil. Ghayebi *et al*. (Ghayebi *et al*., 2022) also used the NDVI index along with other indices to distinguish between the water class of Lake Urmia and the class of non-water areas.

Jeevalakshmi *et al*. (2016) investigated the NDVI index in land cover feature mapping in Andhra Pradesh, India. In this research, in which Landsat-8 images were used, NDVI values were used to classify the four types of water, built-up areas, vegetation and dense vegetation land cover. Fan *et al*. (2015) presented a simple method for rapid and accurate mapping of rubber plantations in Xishuangbanna region in southwest China using a phenology-based vegetation index. In this research, temporal profiles of NDVI, Enhanced Vegetation Index (EVI) and other indices were created using 11 spectral bands of Landsat-8 during one year. The results of this research show the promising potential of the phenology-based vegetation cover index for mapping and monitoring the land surface cover, specifically the spread of rubber on a regional scale.

Aburas *et al*. (2015) studied land cover changes using the NDVI index in another study. This research, while confirming the accuracy and wide application of NDVI in land cover classification, successfully classified land cover without/with vegetation in the Seremban region of Malaysia. Bhandari *et al*. (2012) presented an improved method for analyzing satellite images based on NDVI. This method used remote sensing multi-spectral data technique to find the spectral signature of various objects such as vegetation index, land cover classification, concrete structure, road, urban areas, rocky areas and other areas. The results of the simulations of this research showed that NDVI can be used to detect the surface characteristics of the visible area, which is useful for municipal planning and management. Also, the results showed that

vegetation analysis can be used in the situation of unfortunate natural disasters in order to be used for humanitarian aid, damage assessment, and adopting new strategies.

Land cover mapping is the main factor in studies related to the change of land use/land cover patterns in the world, which is greatly important for sustainable development (Chang *et al*., 2018; Mansourmoghaddam *et al*., 2022b). The present study was conducted to evaluate the accuracy of NDVI index values to map natural land covers, considering the importance of these data in identifying the current state of the land surface as well as changes in different types of land covers at different scales. This evaluation was done with the aim of the feasibility of preparing a natural land cover map and also detecting changes with less cost and time in order to plan as quickly as possible in line with the development and sustainability of the environment. Thus, this makes it possible to obtain land cover maps with relatively favorable accuracy by classifying NDVI index values in the future. The current study examined the precision of the NDVI method in classifying land cover in Iran. It also highlighted the natural classes that are mostly employed in creating land cover maps and added the salt class, which is novel from this perspective and was less obvious in earlier studies.

Material and methods

Study Area

The study area is a part of the Caspian Sea, a part of Iran including Golestan, Mazandaran, Tehran and Semnan provinces, and a part of Turkmenistan. This area is located between 35° to 39° north latitude and 52° to 55° east longitude. The studied area, which has an area of 101,575 km^2, has been selected to include different land cover types such as vegetation, water, barren, salt and agriculture. This area includes Lakes including Gorgan, Miankale, Shoremast, Gol Pol, and Berenjestanak Dam Lake, forests such as Kaboudwall, Pasand and Hyrcanian forests, Haj Ali Qoli salt lake, etc.

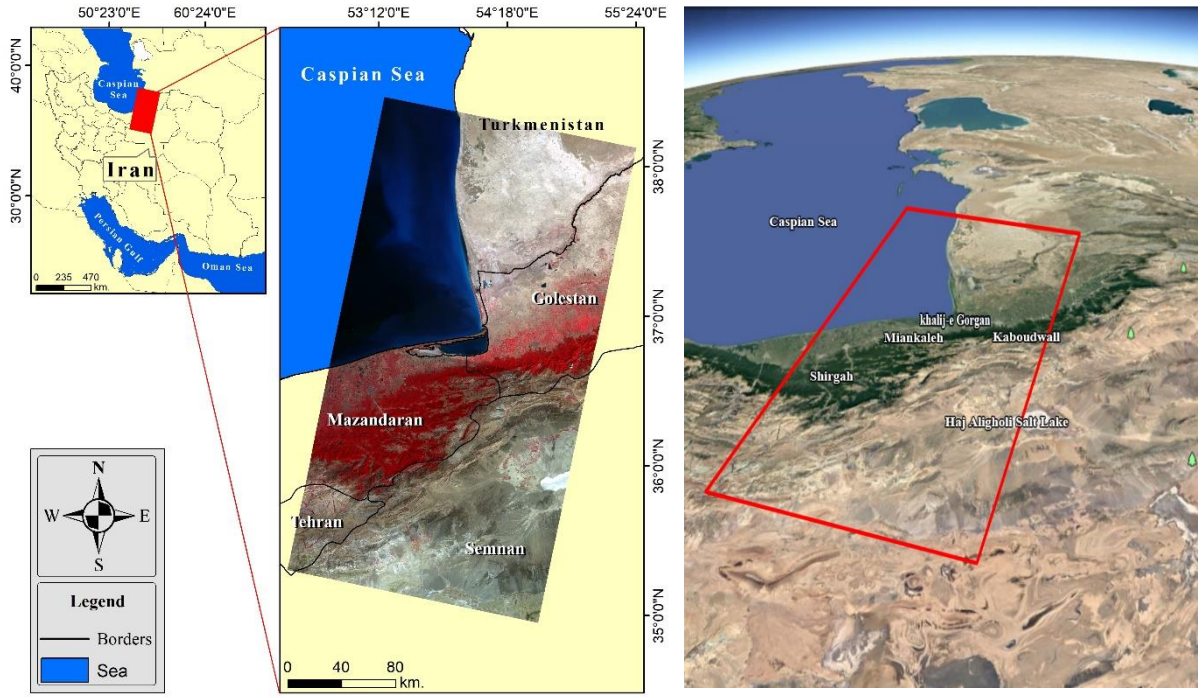

Figure 1. The location of the studied area with its false color composite (5,4,3) Landsat-8 image (left) and its Google Earth image (right)

Data and Materials

In the present study, in order to classify the land cover, two consecutive complete scenes of Landsat-8 on the same date have been used. These images have 9 spectral and 2 thermal bands, and the bands used in this study include blue, green, red, near-infrared, short-wave infrared-1, and short-wave infrared-2 spectral bands with a spatial resolution of 30 meters. The images used were obtained by the United States Geological Survey (www.earthexplorer.usgs.gov). The properties of the images used in this research are listed in Table 1.

Table 1. Characteristics of the images used in the present study

Satellite/Sensor	Image ID	Date	Hour (GMT)	Cloudiness (%)
Landsat-8/OLI	LC08_L1TP_163034_20210830_20210909_02_T1	2021/08/30	07:01:44	0.01
	LC08_L1TP_163035_20210830_20210909_02_T1		07:02:08	0.02

Methodology

Corrections and preprocessing

Before any kind of processing, the images used in the present study were radiometrically corrected for surface reflectance and atmospherically using the FLAASH algorithm, which is recommended for correcting blue areas (Mansourmoghaddam *et al*., 2022a), in the ENVI software environment. Also, according to the type of image received, this image was geometrically corrected and did not need geometric correction.

Image Classification

Maximum Likelihood Classification (MLC)

This classification examines the probability of each pixel belonging to a certain class and then assigns each pixel to a class with the highest membership probability (Hamimi *et al*., 2020). MLC is a technique for assessing the Gaussian Probability Density Function's (PDF) parameters. It operates in a way that the statistical model of choice assigns the observed data as having the highest probability. The Equation (1) may be used to characterize each LU/LC class's fundamental diacritic function (Paola & Schowengerdt, 1995).

$$g_i(X) = p(W|w_i)p(w_i) = \frac{p(\omega_i)}{(2\pi)^{n/2}|\Sigma_i|^{1/2}} * e^{-(1/2)(X-U_i)^T \Sigma_i^{-1}(X-U_i)}, \quad (1)$$

where *n* is the number of bands, *X* is the data vector, *Ui* is the mean vector of the *i*-th class, and Σ_i is the covariance matrix of class *I* defined as the equation (2).

$$X = \begin{bmatrix} x_i \\ x_i \\ \vdots \\ x_n \end{bmatrix} U_i = \begin{bmatrix} \mu_{i1} \\ \mu_{i2} \\ \vdots \\ \mu_{in} \end{bmatrix} \Sigma_i = \begin{bmatrix} \sigma_{i11} & \sigma_{i12} & \cdots & \sigma_{i1n} \\ \sigma_{i21} & \sigma_{i22} & \cdots & \sigma_{i2n} \\ \vdots & \vdots & \ddots & \vdots \\ \sigma_{in1} & \sigma_{in2} & \cdots & \sigma_{inn} \end{bmatrix} \quad (2)$$

The unbiased estimators approximate the values in the mean vector U_i and the covariance matrix Σ_i, from the results of the training:

$$\mu_{ij} = \frac{1}{P}\sum_{l=1}^{P_i} x_{jl} \qquad j = 1,2,\dots,n, \tag{3}$$

$$\sigma_{ijk} = \frac{1}{P}\sum_{l=1}^{P_i}\left(x_{jl} - \mu_{ij}\right)\left(x_{kl} - u_{ik}\right) \qquad j = 1,2,\dots,n; \quad k = 1,2,\dots,n, \tag{4}$$

where P_i represents the number of training patterns in the *i*-th class. Since in this method, it is assumed that all training data have a normal distribution, in order to perform this classification, educational samples were entered into the algorithm as representatives of each class and the classification process was carried out.

Neural Network Classification (NNC)

Artificial neural network or Parallel Distributed Processing (PDP) is known as a system information processor including a large number of interconnected units as processing elements, and is inspired by the biological model (Bischof *et al*., 1992). The artificial neural network is the most widely used classification method (Xiu & Liu, 2003) and is a feed-forward nonlinear layered neural network classification method. The neural network uses the standard backpropagation method for supervised classification. Backpropagation reduces the error between the output and the actual network model and both input and output training examples (Bishop, 1995). In this way, the input/output pair is repeatedly introduced to the network and the error is transferred from the output to the input layer. With the help of a learning rate and an update rule, the backpropagation path weights are updated (Collobert & Weston, 2008). In this method, the performance of the classifier is strongly influenced by the topology of the network such as the number of units and hidden layers and the mutual connections between them (Kadavi & Lee, 2018). The number of hidden layers to use is chosen by the user, and a logistic or hyperbolic activation function can also be chosen. The only communications allowed in the network are forward (such as input to the hidden layer or hidden layer to the output layer (Li *et al*., 2014)). Learning is done in the process of adjusting the weights in each node to reduce the difference between the activation of the output node and the output layer. The error is fed back by the network and the weights are adjusted using a recursive method (Richards, 1999; Exelis Visual Information Solutions Inc, 2015). In order to perform classification by ANN method in ENVI software, the following values are suggested:

Table 2. Suggested values for the input of artificial neural network algorithm (Kavzoglu & Colkesen, 2009)

input	value
Training threshold contribution	0.9
Training momentum field	0.9
Training rate	0.2
Training RMS exit criteria	0.1

Support Vector Machine (SVM)

The SVM method as a set of supervised nonparametric learning methods (Sabins Jr, 1986; Zhang *et al*., 2020) was used for classification. This method isolates the data set by creating a hypermap and provides a logical prediction for the new data set. Since SVM determines the boundary of distinguishing data belonging to two classes from each other in an optimal way based on statistical learning (Huang *et al*., 2002), first, the determination of training samples for each class is done and then the SVM algorithm is used.

Minimum Distance (MinD)

A measure of similarity across distribution functions known as minimal distance classification does not always require that it has all the characteristics of a metric. Any appropriate similarity measure may be referred to as a distance; the term "metric" is used in the conventional mathematical meaning. In this method, first, the average of all classes is determined, then the Euclidean distance of the reflection of each pixel is calculated from the average of all classes (Whiteside *et al*., 2011).

Mahalanobis Distance (MahD)

Image classification based on the Mahalanobis distance method is the same as the minimum distance method, with the difference that in this method, the basis of the classification based on the minimum distance is the minimum Mahalanobis distance and not the minimum Euclidean distance (Yusuf *et al*., 2018). This method was performed assuming the normality of the histogram bands (Shang *et al*., 2020).

Normalized Difference Vegetation Index (NDVI)

NDVI is calculated through the normalized ratio between the red and near-infrared bands (Equation 5) (Avdan & Jovanovska, 2016; Li *et al*., 2017).

$$NDVI = \frac{NIR - R}{NIR + R} \quad (5)$$

Where R represents the red band, band 4 (μm 0.64-0.67) and NIR represents the near-infrared band, band 5 (μm 0.85-0.88) in Landsat-8 (Mansourmoghaddam *et al*., 2021)

Accuracy Assessment

In order to evaluate the performance accuracy of classification algorithms, for each class, nearly a thousand random points scattered based on a combination of geological map, visual interpretation of Google Earth images, and user experience were considered as training samples. 85% of the samples were used in the classification process and 15% of them were used for accuracy evaluation. Then the accuracy was calculated using four accuracy evaluation criteria Overall accuracy, kappa coefficient, producer accuracy and user accuracy (Sexton *et al*., 2013; Ziaul & Pal, 2016) which have been used in many studies to evaluate accuracy (Sexton *et al*., 2013; Ziaul & Pal, 2016; Ishtiaque *et al*., 2017; Sultana & Satyanarayana, 2018; Maleki *et al.*, 2020; Zare Naghadehi *et al*., 2021; Asadi *et al*., 2022; Mansourmoghaddam, *et al*., 2022c). The overall accuracy is the result of dividing all the correctly classified pixels by all the pixels in the N error matrix (Story & Congalton, 1986); The producer's accuracy is calculated by simply dividing the total number of correct pixels in a class by all the pixels in that class obtained from ground reference data (Story & Congalton, 1986). This statistic indicates the probability of a reference pixel being classified in the correct class and is used as a measure of omission error (Jensen, 1996). But if all the correct pixels in a class are divided by the total number of pixels classified in that category, the result will be the Commission error [the error of assigning a pixel to the wrong class]. This measure is called user accuracy or reliability (Story & Congalton, 1986). The Kappa coefficient is also a non-parametric test to determine the degree of compatibility between the actual values and the values assigned by the user (Ishtiaque *et al*., 2017). which is usually used as an index to evaluate the quality of binary feature measurement. When the fit is perfect, the kappa output will be 1 (100 percent), which means that the

classification is true in any context, and a kappa value of 0 means that the fit of the data is no better than a random value. A negative value of Kappa indicates that according to the marginal distribution, the consistency of the data is even lower than a random value. The kappa coefficient depends not only on the sensitivity and unique quality of the two classification classes but also on the correct distribution of the characteristics of the statistical population (Thompson & Walter, 1988).

Results

In order to evaluate the accuracy of the NDVI index in the preparation of the natural land cover map, first, two scenes of the Landsat-8 image including natural water, vegetation, barren land, agricultural land, and salt marsh were classified with different supervised classification methods. These methods included Neural Network Classification (NNC), Maximum Likelihood Classification (MLC), support vector machine (SVM), Minimum Distance (MinD), and Mahalanobis Distance (MahD), that the land cover map was prepared and examined using each one (Figure 2).

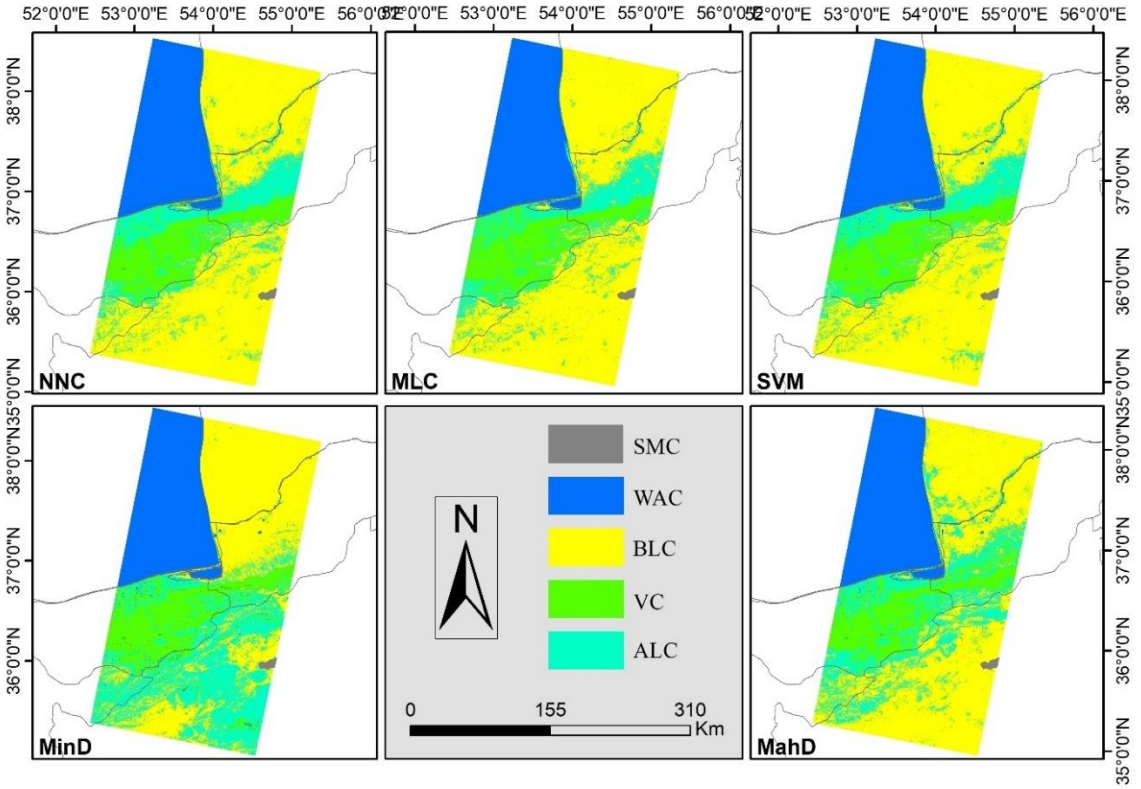

Figure 2. Land cover classification map of the study area with Artificial Neural Network (NNC), Maximum Likelihood (MLC), Support Vector Machine (SVM), Minimum Distance (MinD) and Mahalanobis Distance (MahD) algorithms for Bare Land Class (BLC), Agricultural Land Class (ALC), Vegetation Class (VC), Water Area Class (WAC) and Salt Marsh Class (SMC)

The results of the accuracy evaluation of the land cover map obtained from different classification methods show that the three methods of the MLC, NNC, and SVM with Kappa coefficients of 0.76%, 0.76%, and 0.75% respectively have the most accurate results (Table 3). Among these, the MLC algorithm with the highest accuracy was recognized as the most optimal investigated model.

Table 3. The result of the accuracy assessment (%) of land cover maps prepared by Artificial Neural Network (NNC), Maximum Likelihood (MLC), Support Vector Machine (SVM), Minimum Distance (MinD), and Mahalanobis Distance (MahD) algorithms for Bare Land Class (BLC), Agricultural Land Class (ALC), Vegetation Class (VC), Water Area Class (WAC) and Salt Marsh Class (SMC)

Algorithm	Kappa Coefficient	Overall Accuracy	User Accuracy					Producer Accuracy				
			SMC	WAC	VC	ALC	BLC	SMC	WAC	VC	ALC	BLC
MLC	0.76	80.86	90.7	89.7	89.63	69.14	67.02	92.82	98.67	80.67	73.68	55.26
NNC	0.76	80.86	90.69	87.57	99.19	67.6	68.13	91.72	98.67	81.33	77.63	54.39
SVM	0.75	80.47	90.52	87.06	97.58	70	70	91.69	98.67	80.67	78.29	42.98
MahD	0.67	73.83	89.23	89.87	87.31	52.11	87.1	90.95	94.67	78	73.03	23.68
MinD	0.46	57.03	89.14	87.06	84.56	35.34	47.5	92.94	98.67	76.67	53.95	33.33

After choosing the most optimal model among the studied models, in order to produce the land cover map, the NDVI threshold values were extracted in each of the classes (Table 4).

Table 4. Threshold values of Normalized Difference Vegetation Index (NDVI) in different land cover classes including Bare Land Class (BLC), Agricultural Land Class (ALC), Vegetation Class (VC), Water Area Class (WAC) and Salt Marsh Class (SMC)

Class	NDVI value
BLC	0.036 – 0.19
ALC	0.157 – 0.209
VC	0.301 – 0.911
WAC	-0.811 – -0.033
SMC	0.133 – 0.157

After extracting the NDVI threshold values in the natural land cover classes investigated in this research, the land cover classification map obtained from the classification of NDVI values was obtained (Figure 3-left). This map will be called NDVI Based Classification (NBC) from now on.

Based on the results obtained from the validation of the NBC, the land cover map has been extracted with an overall accuracy of 83% and a kappa coefficient of 77%. NDVI has shown good performance in the classification of BLC, WAC and SMC with user accuracy and producer accuracy of above 94%. This is while the ALC and VL are classified by this index with producer accuracy of 73% and user accuracy of 69% and 97%, respectively (Table 5).

Comparing the accuracy of the land cover map obtained from the most optimal method, MLC and the obtained NDVI value-based land cover map (NBC) shows that in NBC classification, the overall accuracy and Kappa coefficient increase by 1.79 and 1.11, respectively. The user accuracy has also increased by 30.3, 7.7, 4.6, and 2.4 in the BLC, VC, WAC, and SMC, respectively, and decreased by 0.1 in the ALC. In this comparison, the producer accuracy increased by 43.9, 0.1, and 4.5 in the BLC, ALC, and SMC, respectively, and decreased by 6.8 and 3.7 in the VC and WAC, respectively (Figure 4).

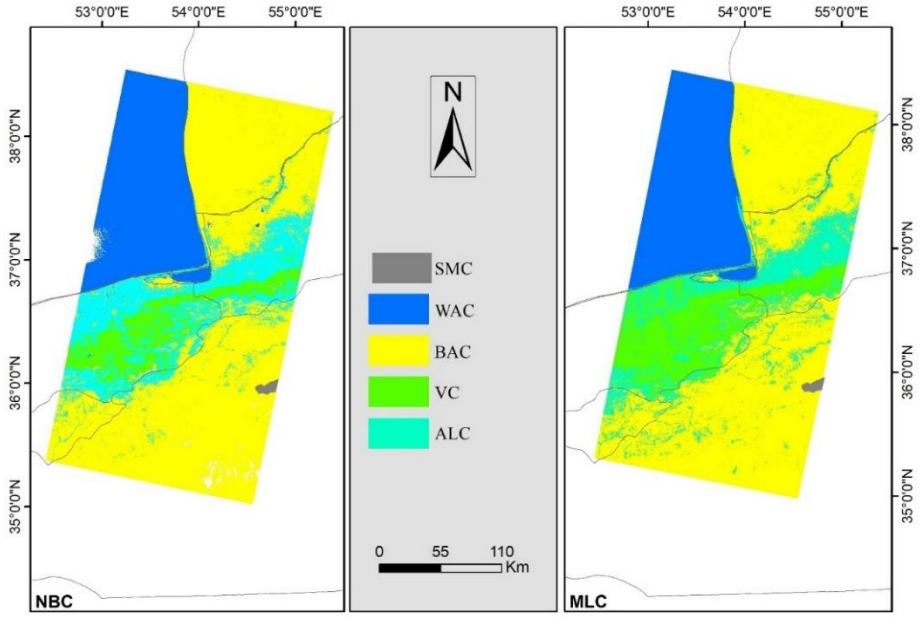

Figure 3. Comparison of the output of land cover classification obtained from the Maximum Likelihood (MLC) algorithm and the classification based on the NDVI Based Classification (NBC) for Bare Land Class (BLC), Agricultural Land Class (ALC), Vegetation Class (VC), Water Area Class (WAC) and Salt Marsh Class (SMC)

Table 5. The results of the accuracy assessment of the obtained land cover classification map based on the Normalized Difference Vegetation Index (NBC)

Algorithm	Kappa Coefficient	Overall Accuracy	User Accuracy					Producer Accuracy				
			SMC	WAC	VC	ALC	BLC	SMC	WAC	VC	ALC	BLC
NBC	0.77	82.65	94.92	94.34	97.35	68.99	97.35	97.3	95.01	73.83	73.83	99.12

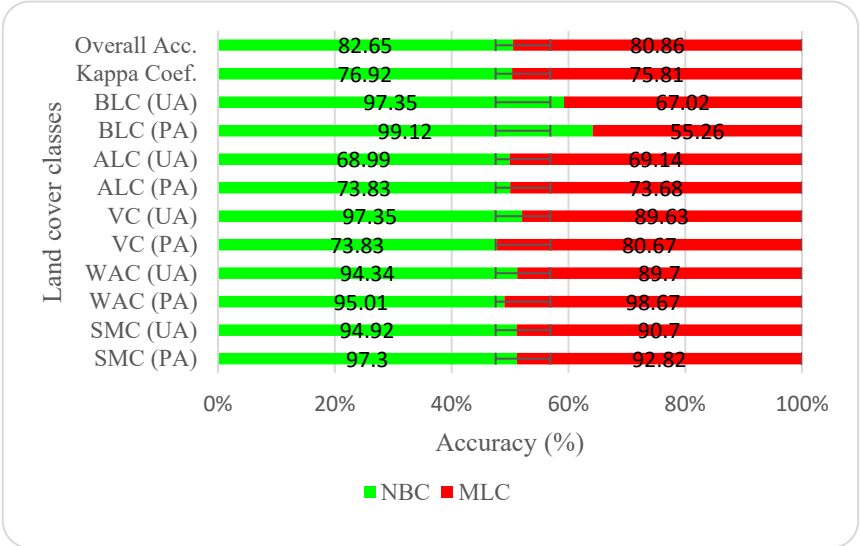

Figure 4. Comparison of the Kappa Coefficient, Overall accuracy, User Accuracy (UA) and Producer Accuracy (PA) of land cover classification obtained from the Maximum Likelihood (MLC) algorithm and the classification based on the NDVI Based Classification (NBC) for Bare Land Class (BLC), Agricultural Land Class (ALC), Vegetation Class (VC), Water Area Class (WAC) and Salt Marsh Class (SMC)

Discussion

The sustainable development of the environment is one of the most important issues in the world and one of the most critical studies in this field is the investigation of land cover changes, one of the leading ways of which is to prepare land cover maps from remote sensing data (Turner *et al*. al., 1995; Chang *et al*., 2018). The present study was conducted to evaluate the accuracy of land cover classification produced based on NDVI values in order to facilitate and accelerate the preparation of natural land cover maps. For this purpose, firstly, each classification algorithm's accuracy including NNC, MLC, SVM, MinD, and MahD was assessed in five classes BLC, ALC, WAC, SMC, and VC. The results of this research showed that the MLC with an overall accuracy of 80.86% and a Kappa coefficient of 75.81 showed the most optimal results in terms of accuracy. This part of the results, with the previous studies that as the most optimal algorithm, to classify multi-spectral remote sensing images using this algorithm (Wei & Mendel, 2000; Dean & Smith, 2003; Ahmad & Quegan, 2012) or to compare the accuracy (Strahler, 1980; DeFries & Townshend, 1994) were also consistent. Then the NDVI values were thresholded based on the MLC land cover map. Based on this, values from 0.036 to 0.19 correspond to BLC, values from 0.147 to 0.209 correspond to ALC, values from 0.301 to 0.911 correspond to VC, values from -0.811 to -0.033 related to WAC and values from 0.133 to 0.168 related to SMC were detected. The results of evaluating the accuracy of NBC indicate that this index with an overall accuracy of 82.65% and a kappa coefficient of 76.92% was able to show an acceptable result and even more accurate than MLC. In NBC, user accuracy in BLC by 30.3, VC by 7.7, WAC by 4.6, and SMC by 4.2 has increased. Producer accuracy has also by 43.9 in BLC, by 0.1 in ALC, and by 44.5 in SMC increased. which indicates the acceptable accuracy of the NDVI value in separating and classifying natural studied land cover classes and the results of some previous studies, such as (DeFries & Townshend, 1994; Stathopoulou *et al*., 2007; Aburas *et al*., 2015; Jeevalakshmi *et al*., 2016) also, directly and indirectly, confirm these results.

Conclusion

The present study was conducted to evaluate the accuracy of natural land cover classification based on NDVI values thresholding to facilitate the preparation of land cover maps, which is one of the important tools in planning and environmental development and sustainability studies. First of all, the examination of the most well-known classification algorithms showed that the MLC algorithm was more accurate. The results of this research showed that classification based on NDVI values thresholding had acceptable results in extracting five classes of BLC, ALC, VC, WAC, and SMC. Also, the results showed that compared to other supervised algorithms, the classification based on NDVI value had increased the producer accuracy in the BLC, ALC, and SMC and the user accuracy in the BLC, VC, WAC, and SMC. The present study investigated the accuracy of the NDVI algorithm in the classification of land cover in Iran and also discussed the natural classes that are mainly used in the preparation of land cover maps and also included the salt class in this classification, which is innovative from this point of view and are less found in the previous research. The results of this research will be suitable for researchers, monitors and environmental planners, and scientists related to monitoring and investigating land cover changes in order to use NDVI to prepare land cover maps with less cost and time.

References

Aburas M. M., S. H. Abdullah, M. F. Ramli, & Z. H. Ash'aari, 2015. Measuring land cover change in Seremban, Malaysia using NDVI index. Procedia Environmental Sciences, 30; 238-243.

Ahmad, A., & S. Quegan, 2012. Analysis of maximum likelihood classification on multispectral data. Applied Mathematical Sciences, 6(129); 6425-6436.

Ahmadi, H., & A. Nusrath, 2010. Vegetation change detection of Neka River in Iran by using remote-sensing and GIS. Journal of geography and geology, 2(1); 58.

Alavipanah, S. K., M. Karimi Firozjaei, M., Sedighi, A., Fathololoumi, S., Zare Naghadehi, S., Saleh, S., & P. M.Atkinson, 2022. The Shadow Effect on Surface Biophysical Variables Derived from Remote Sensing: A Review. Land, 11(11); 1-30.

Asadi M, Oshnooei-Nooshabadi A, Saleh Sa, Habibnezhad F, Sarafraz-Asbagh S, Van Genderen JL, 2022. Simulation of Urban Sprawl by Comparison Cellular Automata-Markov and ANN. ??????

Avdan, U., & G. Jovanovska, 2016. Algorithm for automated mapping of land surface temperature using LANDSAT 8 satellite data. Journal of Sensors, 2016; 1-8.

Bhandari, A., A. Kumar, & G. Singh, 2012. Feature extraction using Normalized Difference Vegetation Index (NDVI): A case study of Jabalpur city. Procedia technology, 6; 612-621.

Bischof, H., W. Schneider, & A. J. Pinz, 1992. Multispectral classification of Landsat-images using neural networks. IEEE Transactions on Geoscience and Remote Sensing, 30(3); 482-490.

Bishop, C. M., 1995. Neural networks for pattern recognition. Oxford University Press.

Chang, Y., K. Hou, X. Li, Y. Zhang, & P. Chen. (2018). Review of land use and land cover change research progress. IOP Conference Series: Earth and Environmental Science. pp. 12-87

Collobert, R., & J. Weston. (2008). A unified architecture for natural language processing: Deep neural networks with multitask learning. Proceedings of the 25th international conference on Machine learning. pp, 160-167.

Dean, A., & G. Smith, 2003. An evaluation of per-parcel land cover mapping using maximum likelihood class probabilities. International Journal of Remote Sensing, 24(14); 2905-2920.

DeFries, R. S., & J. Townshend, 1994. NDVI-derived land cover classifications at a global scale. International Journal of Remote Sensing, 15(17); 3567-3586.

Exelis Visual Information Solutions Inc, 2015. ENVI 5.3 help.

Fan, H., X. Fu, Z. Zhang, & Q. Wu, 2015. Phenology-based vegetation index differencing for mapping of rubber plantations using Landsat OLI data. Remote Sensing, 7(5); 6041-6058.

Ghayebi, A., A. Ahmadi, & B. Bigdeli, 2022. Investigating the surface changes of Urmia Lake using the integration of Landsat-8 and Sentinel-2 satellite data. Journal of RS and GIS for Natural Resources.

Hacihaliloglu, I., & M. Karta. (2004). DCT and DWT based image compression in remote sensing images. IEEE Antennas and Propagation Society Symposium, 2004; 3856-3858.

Hamimi, Z., W. Hagag, S. Kamh, & A. El-Araby, 2020. Application of remote-sensing techniques in geological and structural mapping of Atalla Shear Zone and Environs, Central Eastern Desert, Egypt. Arabian Journal of Geosciences, 13(11); 1-27.

Huang, C., L. Davis, & J. Townshend, 2002. An assessment of support vector machines for land cover classification. International Journal of remote sensing, 23(4); 725-749.

Ishtiaque, A., M. Shrestha, & N. Chhetri, 2017. Rapid urban growth in the Kathmandu Valley, Nepal: Monitoring land use land cover dynamics of a himalayan city with landsat imageries. Environments, 4(4); 1-16.

Jeevalakshmi, D., S. N. Reddy, & B. Manikiam. (2016). Land cover classification based on NDVI using LANDSAT8 time series: A case study Tirupati region. 2016 International Conference on Communication and Signal Processing (ICCSP). pp. 1332-1335.

Jensen, J. R., 1996. Introductory digital image processing: a remote sensing perspective. Prentice-Hall Inc.

Kadavi, P. R., & C.-W. Lee, 2018. Land cover classification analysis of volcanic island in Aleutian Arc using an artificial neural network (ANN) and a support vector machine (SVM) from Landsat imagery. Geosciences Journal, 22(4); 653-665.

Kavzoglu, T., & I. Colkesen, 2009. A kernel functions analysis for support vector machines for land cover classification. International Journal of Applied Earth Observation and Geoinformation, 11(5); 352-359.

Li, C., J. Wang, L. Wang, L. Hu, & P. Gong, 2014. Comparison of classification algorithms and training sample sizes in urban land classification with Landsat thematic mapper imagery. Remote Sensing, 6(2); 964-983.

Li, X., Y. Zhou, G. R. Asrar, M. Imhoff, & X. Li, 2017. The surface urban heat island response to urban expansion: A panel analysis for the conterminous United States. Science of the Total Environment, 605; 426-435.

Maleki M., J.L. Van Genderen, S.M. Tavakkoli-Sabour, S.S. Saleh, E. Babaee, 2020. Land use/cover change in Dinevar rural area of West Iran during 2000–2018 and its prediction for 2024 and 2030. Geogr.Tech., 15; 93-105.

Mansourmoghaddam, M., H. R. Ghafarian Malamiri, I. Rousta, H. Olafsson, & H. Zhang, 2022a. Assessment of Palm Jumeirah Island's Construction Effects on the Surrounding Water Quality and Surface Temperatures during 2001–2020. Water, 14(4); 1-16.

Mansourmoghaddam, M., H. R. Ghafarian Malamiri, F. Arabi Aliabad, M. Fallah Tafti, M. Haghani, & S. Shojaei, 2022b. The Separation of the Unpaved Roads and Prioritization of Paving These Roads Using UAV Images. Air, Soil and Water Research, 15; 1-10.

Mansourmoghaddam M., I. Rousta, M. S. Zamani, M. H. Mokhtari, M. Karimi Firozjaei, S. K. Alavipanah. 2022c. Investigating And Modeling the Effect of The Composition and Arrangement of The Landscapes of Yazd City on The Land Surface Temperature Using Machine Learning and Landsat-8 and Sentinel-2 Data. Iranian Journal of Remote Sensing & GIS, 15(3).

Mansourmoghaddam, M., I. Rousta, M. Zamani, M. H. Mokhtari, M. Karimi Firozjaei, & S. K. Alavipanah, 2021. Study and prediction of land surface temperature changes of Yazd city: assessing the proximity and changes of land cover. Journal of RS and GIS for Natural Resources, 12(4); 1-27.

Mohammadnazhad, P., M. Moameri, A. Ghorbani, F. Dadjou, & V. Mohammadi, 2022. Modeling aboveground net primary production using Landsat-8 indices in Siahpoosh and Ganjgah rangelands of Ardabil province, Iran. Journal of RS and GIS for Natural Resources, 14(3); 13-16.

Paola JD., R. A. Schowengerdt, 1995. A detailed comparison of backpropagation neural network and maximum-likelihood classifiers for urban land use classification. IEEE Transactions on Geoscience, 33(4); 981-996.

Richards, J.A., 1999. Remote Sensing Digital Image Analysis Berlin: Springer-Verlag; p. 240.

Rouse Jr, J. W., R. H. Haas, J. Schell, & D. Deering. (1973). Monitoring the vernal advancement and retrogradation (green wave effect) of natural vegetation (No. E75-10354).

Sabins Jr, F. F. (1986). Remote sensing: principles and interpretation; p. 280-289.

Sexton, J. O., D. L. Urban, M. J. Donohue, & C. Song, 2013. Long-term land cover dynamics by multi-temporal classification across the Landsat-5 record. Remote sensing of environment, 128; 246-258.

Shang, S., K.-N. He, Z.-B. Wang, T. Yang, M. Liu, & X. Li, 2020. Sea clutter suppression method of HFSWR based on RBF neural network model optimized by improved GWO algorithm. Computational Intelligence and Neuroscience, 2020; 1-10.

Silakhori, E., & M. Ownegh, 2018. Identification and differentiating of geomorphology facies of Sabzevar region using Remote sensing and GIS. Journal of RS and GIS for Natural Resources, 9(1); 113-130.

Stathopoulou, M., C. Cartalis, & M. Petrakis, 2007. Integrating Corine Land Cover data and Landsat TM for surface emissivity definition: application to the urban area of Athens, Greece. International Journal of Remote Sensing, 28(15); 3291-3304.

Story, M., & R. G. Congalton, 1986. Accuracy assessment: a user's perspective. Photogrammetric Engineering and remote sensing, 52(3); 397-399.

Strahler, A. H., 1980. The use of prior probabilities in maximum likelihood classification of remotely sensed data. Remote sensing of Environment, 10(2); 135-163.

Taufik, A., S. S. S. Ahmad, & A. Ahmad, 2016. Classification of landsat 8 satellite data using NDVI tresholds. Journal of Telecommunication, Electronic and Computer Engineering (JTEC), 8(4); 37-40.

Thompson, W. D., & S. D. Walter, 1988. A reappraisal of the kappa coefficient. Journal of clinical epidemiology, 41(10); 949-958.

Turner, B. L., D. Skole, S. Sanderson, G. Fischer, L. Fresco, & R. Leemans, 1995. Land-use and land-cover change: science/research plan. [No source information available].

Wei, W., & J. M. Mendel, 2000. Maximum-likelihood classification for digital amplitude-phase modulations. IEEE transactions on Communications, 48(2); 189-193.

Whiteside, T. G., G. S. Boggs, & S. W. Maier, 2011. Comparing object-based and pixel-based classifications for mapping savannas. International Journal of Applied Earth Observation and Geoinformation, 13(6); 884-893.

Xiu, L.-n., & X.-n. Liu, 2003. Current status and future direction of the study on artificial neural network classification processing in remote sensing. Remote Sensing Technology and Application, 18(5); 339-345.

Yusuf, F. R., K. B. Santoso, M. U. L. Ningam, M. Kamal, & P. Wicaksono. (2018). Evaluation of atmospheric correction models and Landsat surface reflectance product in Daerah Istimewa Yogyakarta, Indonesia. IOP Conference Series: Earth and Environmental Science, 169; 1-10.

Zare Naghadehi S., M. Asadi, M. Maleki, S. M. Tavakkoli-Sabour, J.L. Van Genderen, S.S. Saleh, 2021. Prediction of Urban Area Expansion with Implementation of MLC, SAM and SVMs' Classifiers Incorporating Artificial Neural Network Using Landsat Data. ISPRS International Journal of Geo Information, 10(8); 1-16.

Zhang, J., C. Lu, J. Wang, X.-G. Yue, S.-J. Lim, Z. Al-Makhadmeh, & A. Tolba, 2020. Training convolutional neural networks with multi-size images and triplet loss for remote sensing scene classification. Sensors, 20(4); 1-21.

Ziaul, S., Pal S. 2016. Image based surface temperature extraction and trend detection in an urban area of West Bengal, India. Journal of Environmental Geography, 9(3-4); 13-25.